Bioresource Technology 323 (2021) 124573

Contents lists available at ScienceDirect

Bioresource Technology

journal homepage: www.elsevier.com/locate/biortech

Blending industrial blast furnace gas with H_2 enables *Acetobacterium woodii* to efficiently co-utilize CO, CO_2 and H_2

Katharina Novak [a], Christian Simon Neuendorf [a], Irmela Kofler [b], Nina Kieberger [c], Steffen Klamt [d], Stefan Pflügl [a,*]

[a] Technische Universität Wien, Institute for Chemical, Environmental and Bioscience Engineering, Research Area Biochemical Engineering, Gumpendorfer Straße 1a, 1060 Vienna, Austria
[b] K1-MET GmbH, Stahlstraße 14, 4020 Linz, Austria
[c] voestalpine Stahl GmbH, voestalpine-Straße 3, 4020 Linz, Austria
[d] Max Planck Institute for Dynamics of Complex Technical Systems, 39106 Magdeburg, Germany

HIGHLIGHTS

- *A. woodii* can utilize industrial blast furnace gas for growth and acetate production.
- CO, CO_2 and H_2 can be co-utilized in batch and continuous cultivation.
- Maximum specific H_2 uptake rate of *A. woodii* is between 116 and 167 mmol $g^{-1}h^{-1}$.
- Blending blast furnace gas with H_2 enables acetate production at 14 mmol $l^{-1}h^{-1}$.
- Blending industrial gas with H_2 allows control of gas uptake and carbon distribution.

GRAPHICAL ABSTRACT

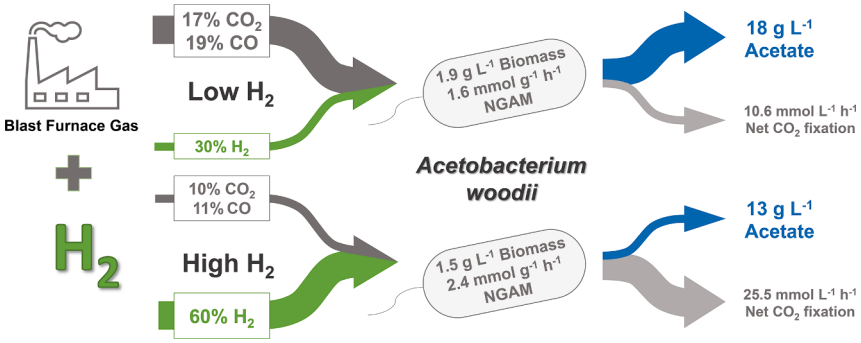

ARTICLE INFO

Keywords:
Industrial CO_2 emissions
Acetogens
Net CO_2 fixation
Mixed gas fermentation
Maximum specific hydrogen uptake rate

ABSTRACT

In this study, the impact of gas composition (i.e. CO, CO_2 and H_2 partial pressures) on CO_2 utilization, growth, and acetate production was investigated in batch and continuous cultures of *A. woodii*. Based on an industrial blast furnace gas, H_2 blending was used to study the impact of H_2 availability on CO_2 fixation alone and together with CO using idealized gas streams. With H_2 available as an additional energy source, net CO_2 fixation and CO, CO_2 and H_2 co-utilization was achieved in gas-limited fermentations. Using industrial blast furnace gas, up to 15.1 g l^{-1} acetate were produced in continuous cultures. Flux balance analysis showed that intracellular fluxes and total ATP production were dependent on the availability of H_2 and CO. Overall, H_2 blending was shown to be a suitable control strategy for gas fermentations and demonstrated that *A. woodii* is an interesting host for CO_2 fixation from industrial gas streams.

* Corresponding author.
E-mail addresses: katharina.novak@tuwien.ac.at (K. Novak), christian.neuendorf@tuwien.ac.at (C.S. Neuendorf), irmela.kofler@k1-met.com (I. Kofler), nina.kieberger@voestalpine.com (N. Kieberger), klamt@mpi-magdeburg.mpg.de (S. Klamt), stefan.pfluegl@tuwien.ac.at (S. Pflügl).

https://doi.org/10.1016/j.biortech.2020.124573
Received 15 November 2020; Received in revised form 14 December 2020; Accepted 15 December 2020
Available online 28 December 2020

1. Introduction

The use of CO_2 as a substrate is one possibility to reduce atmospheric CO_2 emissions, close global carbon cycles and to establish a circular economy (Bengelsdorf and Dürre, 2017; Liew et al., 2016b; Vees et al., 2020). One of the biggest industrial CO_2 emitters is the iron and steel industry, which accounts for 5% of anthropogenic CO_2 emission in the European Union ("Eurostat,", 2018; Pardo and Moya, 2013). A variety of process gases are produced during the production process and blast furnace gas (BFG), formed during the reduction of iron ore to iron is one example for a by-product gas from the steel milling process (Hou et al., 2011; Molitor et al., 2016). Hydrogen is an important energy source for acetogenic gas fermentations and a promising future electron carrier that can be obtained from renewable resources (Das and Veziroglu, 2008; Hallenbeck and Ghosh, 2009; Yukesh Kannah et al., 2021).

Acetogenic bacteria are promising microbial hosts for industrial CO_2 fixation since they have the ability to fix carbon in the form of CO and CO_2 via the Wood-Ljungdahl pathway (WLP), where two molecules of CO_2 are reduced to acetyl-CoA using H_2 as an energy source (Bertsch and Müller, 2015a; Köpke and Simpson, 2020; Schoelmerich and Müller, 2020; Schuchmann and Müller, 2014). Acetate is the main product of acetogens, but the product spectrum of different acetogenic strains is broad and includes ethanol, 2,3-butanediol, butanol, butyrate and others (Liew et al., 2016b). Chemical production using acetogens therefore is a promising alternative to energy intensive chemical processes such as the Fisher-Tropsch synthesis (Munasinghe and Khanal, 2010; Takors et al., 2018). An industrial process for ethanol production from CO using *Clostridium autoethanogenum* has already been commercialized by the leading company LanzaTech Inc (Skokie, IL, USA).

Acetobacterium woodii is a homoacetogenic bacterium known to efficiently utilize CO_2 and H_2 (Kantzow et al., 2015; Schuchmann and Müller, 2014). In addition to autotrophic growth, *A. woodii* can utilize a broad variety of substrates including C1 components such as formate and methanol (Drake et al., 1997; Schuchmann and Müller, 2016; Wiechmann et al., 2020). During growth on H_2 and CO_2, 0.3 mol ATP are formed per mol of acetate produced (Schuchmann and Müller, 2014). This low ATP gain allows *A. woodii* to grow at very low H_2 partial pressures and explains why cultivation on H_2 and CO_2 is much easier compared to *C. autoethanogenum*, which has a higher H_2 threshold (Mock et al., 2015). *A. woodii* was the first organism where energy conservation was fully elucidated (Schuchmann and Müller, 2014) and additional metabolic properties continue to be described (Westphal et al., 2018; Wiechmann et al., 2020). Acetate produced by *A. woodii* can either be used directly or upgraded into other valuable products (Novak et al., 2020; Novak and Pflügl, 2018). The production of acetate is advantageous over a mixed product spectrum due to controllability of the process (Schwarz et al., 2020). Growth and acetate production on CO_2 and H_2 have been characterized in detail (Demler and Weuster-Botz, 2011; Kantzow et al., 2015) and the mechanism of CO utilization has been described (Arantes et al., 2020; Bertsch and Müller, 2015b; Schwarz et al., 2020), but data on utilization of gas containing both CO and CO_2 is scarce. The presence of CO inhibits bacterial hydrogenases, in particular the hydrogen-dependent CO_2 reductase (HDCR) (Bertsch and Müller, 2015b; Ragsdale and Ljungdahl, 1984), which leads to delayed growth in the presence of CO. However, growth can be restored by the addition of formate, the product of the HDCR (Bertsch and Müller, 2015b). Although initially reported to grow on CO as the sole carbon and energy source, it has recently been shown that *A. woodii* does not grow on CO alone (Bertsch and Müller, 2015b; Genthner and Bryant, 1987).

In contrast to *A. woodii*, CO utilization of several clostridial species has been broadly studied, owing to their enhanced CO utilization properties (Cotter et al., 2009; Mahamkali et al., 2020; Mohammadi et al., 2012; Valgepea et al., 2018, 2017). Special attention has been given to the utilization of synthesis gas, which contains large amounts of CO and H_2 as well as CO_2 in varying minor quantities (Takors et al., 2018). Compared to CO_2 and H_2, growth of *Clostridium ljungdahli* and *C. autoethanogenum* on CO shows higher growth rates, increased ATP generation and the production of reduced compounds such as ethanol (Hermann et al., 2020; Mahamkali et al., 2020). However, CO utilization is usually accompanied by CO_2 production, which has been reduced by the additional supply of H_2 to CO-grown *C. autoethanogenum* (Valgepea et al., 2018). The addition of H_2 also shifted the product spectrum towards more reduced end products, highlighting that the feed gas composition can be considered a critical factor for enhancing the economics of gas fermentation processes. A recent study has shown that the addition of 2% CO enhanced fermentation of CO_2 and H_2 in *C. autoethanogenum* (Heffernan et al., 2020), while utilization of syngas containing high amounts of CO resulted in the formation of CO_2 (Valgepea et al., 2018, 2017).

Due to the toxicity mechanisms of CO, a process focussing on CO_2 fixation in CO-containing gas (e.g. BFG) needs to aim for limitation of CO in the liquid medium to achieve co-utilization of CO, CO_2 and H_2. This CO limitation can be achieved due to low solubility of CO in combination with high biomass and thereby high CO uptake rates (Bertsch and Müller, 2015a).

This study aimed to determine the effect of the gas composition (i.e. CO, CO_2 and H_2 partial pressures) on CO_2 utilization, growth, and acetate production in *A. woodii*. Considering the gas composition of industrial BFG as a starting point, idealized gases with and without CO blended with different concentrations of H_2 were used. This approach allowed to draw conclusions about effects on growth and acetate formation mediated by both H_2 and CO availability. Moreover, it was hypothesized that H_2 blending could also be a useful tool to enable co-utilization of CO, CO_2 and H_2 and net CO_2 fixation. Indeed, H_2 blending and limitation of the inhibitory gas CO in continuous cultures enabled *A. woodii* to efficiently produce acetate from industrial BFG. Using a metabolic model, the effect of gas composition on intracellular carbon, redox and energy metabolism was studied. The gas fermentation strategy used here provides valuable information on acetogenic metabolism and shows potential in upgrading industrial gas pollutants into value-added products.

2. Materials and methods

2.1. Organism and media

Acetobacterium woodii DSM 1030 was obtained from DSMZ (German Collection of Microorganisms and Cell Cultures GmbH, Braunschweig, Germany) and used for all cultivations.

The medium for all cultivations is based on media 135 suggested by DSMZ. Changes in the medium included omitting Na_2S * 9 H_2O and an increase in Ca-pantothenate and $FeSO_4$*7 H_2O. Bicarbonate-buffered medium was used for the initial experiments in serum bottles investigating growth on BFG. This medium was later replaced by phosphate-buffered medium which was used in serum bottle experiments investigating the effect of formate and for all bioreactor cultivations. Bicarbonate-buffered medium contained per liter: 1 g NH_4Cl, 0.1 g $MgSO_4{\cdot}7H_2O$, 2 g yeast extract, 0.33 g KH_2PO_4, 0.45 g K_2HPO_4, 0.5 g cysteine-HCl·H_2O, 10 g $NaHCO_3$, 0.25 ml sodium resazurin (0.2% w/v), 20 ml trace element solution DSMZ 141, and 10 ml vitamin solution DSMZ 141. In phosphate-buffered serum bottle medium $NaHCO_3$ was replaced by 1.76 g l^{-1} KH_2PO_4, 8.44 g l^{-1} K_2HPO_4 and 3.47 g l^{-1} NaCl. For mixotrophic precultures, 5 g l^{-1} fructose or formate were added from anoxic sterile stocks of 250 g l^{-1}. The trace element solution was adapted from medium DSMZ 141 and contained per liter: 1.5 g nitrilotriacetic acid, 3 g $MgSO_4$ * 7 H_2O, 0.5 g $MnSO_4{\cdot}H_2O$, 1 g NaCl, 0.1 g $FeSO_4$ * 7 H_2O, 0.152 g $Co(II)Cl_2$ * 6 H_2O, 0.1 g $CaCl_2$ * 2 H_2O, 0.18 g $ZnSO_4$ * 7 H_2O, 0.01 g $CuSO_4$ * 5 H_2O, 0.02 g $KAl(SO_4)_2$ * 12 H_2O, 0.01 g boric acid, 0.01 g Na_2MoO_4 * 2 H_2O, 0.033 g $Ni(II)SO_4$ * 6 H_2O, 0.3 mg Na_2SeO_3 * 5 H_2O and 0.4 mg Na_2WO_4 * 2 H_2O. The vitamin solution was prepared according to DSMZ medium 141 and contained per liter: 2 mg biotin, 2 mg folic acid, 10 mg pyridoxine-HCl, 5 mg thiamine-HCl, 5 mg riboflavin,

5 mg nicotinic acid, 5 mg D-Ca-pantothenate, 0.1 mg vitamin B12, 5 mg *para*-aminobenzoic acid and 5 mg lipoic acid. The pH of all media was adjusted to 7.0 using 5 M KOH. For bioreactor cultivations, the media composition was adapted: concentration of the phosphate buffer was reduced to 0.33 g KH_2PO_4 and 0.45 g K_2HPO_4, trace element and vitamin concentrations (except for Ca-pantothenate which was added to a concentration of 1 mg l^{-1} in the final medium according to (Godley et al., 1990)) were doubled and the iron concentration was increased to 26.9 mg l^{-1} $FeSO_4$*7 H_2O in the final medium (Demler and Weuster-Botz, 2011).

Media was prepared using anaerobic techniques as described previously (Hungate, 1969). All chemicals were purchased from Roth (Carl Roth GmbH + Co. KG, Karlsruhe, Germany) or Merck (Merck KGaA, Darmstadt, Germany).

2.2. Gases and compositions

Premixed gas containing 80% H_2 and 20% CO_2 was obtained from Air Liquide Austria GmbH (Schwechat, Austria) and used for routine cultivations such as precultures. Industrial blast furnace gas (BFG) was filled into gas cylinders directly on site at the blast furnace of voestalpine Stahl GmbH (Linz, Austria). The gas composition represents the annual average of the online quantification by the multi-analysis-system Advance Optima AO2000 (ABB Asea Brown Boveri Ltd, Zürich, Switzerland).

BFG was blended with H_2 (Messer Austria GmbH, Gumpoldskirchen, Austria) to obtain H_2 concentrations of 30% (low H_2 blend) and 60% (high H_2 blend) using two independent mass flow controllers (Eppendorf AG, Hamburg, Germany and CRANE Instrumentation & Sampling, Spartanburg, SC, USA). Idealized gases with and without CO containing the same amount of CO_2, CO and H_2 as the corresponding BFG-H_2 blend were purchased from Messer Austria GmbH (Gumpoldskirchen, Austria).

2.3. Preparation of precultures

A. woodii was stored as anoxic stocks at −80 °C in 125 g l^{-1} saccharose. For cultivations, these stocks were transferred into 125 ml serum bottles containing 50 ml medium with 5 g l^{-1} fructose. For mixotrophic growth, the atmosphere was exchanged to 80% H_2 and 20% CO_2 and a total pressure of 2.5 bar was applied. *A. woodii* was cultivated in a rotary shaker at 30 °C and 200 rpm (Infors AG, Bottmingen, Switzerland). For further cultivation in serum bottles, 2 ml of the mixotrophic culture was transferred anaerobically to fresh medium. Batch experiments in bioreactors were inoculated with an exponentially growing culture obtaining an optical density at 600 nm (OD_{600}) of 0.1. For cultivations on gas without CO mixotrophic precultures were used, whereas cultivations on gas containing CO were inoculated with a preculture previously grown on 5 g l^{-1} formate and the high H_2 blend of the BFG.

2.4. Experiments in serum bottles

Growth experiments in 125 ml serum bottles were carried out using 50 ml medium. During the initial experiments for growth on the industrial flue gas, bicarbonate-buffered medium was used and later replaced by phosphate-buffered medium for experiments with formate. The atmosphere in the head space was exchanged by the desired gas composition and pressurized with a total pressure of 2.5 bar. The industrial flue gas was diluted with H_2 using two mass flow controllers (Brooks Instrument, Matfield, USA). Upon gas consumption, the headspace was refilled with the corresponding gas at 1.5 bar. Samples of 2 ml were regularly taken and used for OD_{600} and high-performance liquid chromatography (HPLC) measurements.

2.5. Cultivations in bioreactors

Bioreactor cultivations were carried out in duplicates in a DASbox® Mini Bioreactor system (Eppendorf AG, Hamburg, Germany) with a working volume of 200 ml at a temperature of 30 °C. The pH was initially set to 7.0, monitored by a pH electrode EasyFerm Plus K8 120 (Hamilton, Reno, NV, USA) and controlled by the addition of 2 M phosphoric acid and 5 M KOH with a MP8 multi pump module (Eppendorf AG, Hamburg, Germany). The agitator speed was routinely set to 600 rpm and adjusted to 300 and 1200 rpm to investigate gas liquid mass transfer. In both batch and continuous cultures, the medium was continuously sparged with 0.25 vvm (3 sl h^{-1}) of the indicated gas. Microspargers made of sintered metal with a pore size of 10 μm (Sartorius Stedim Biotech GmbH, Göttingen, Germany) were used for improved gas transfer into the liquid phase. Prior to inoculation, the reactor medium was flushed with the appropriate gas for at least 3 h. During continuous cultivations, feed medium and a 1% (w/v) solution of antifoam (Struktol SB2020, Schill und Seilacher, Hamburg, Germany) were continuously added with the MP8 pump module at a rate of 10 ml h^{-1} and 0.2 ml h^{-1}, respectively. To keep the reaction volume constant, culture broth was continuously removed by peristaltic pumps (Ismatec SA, Glattburg, Germany) via a dip tube and the cultivation volume was maintained at 197 ± 11 ml. The feed bottles were continuously flushed with 6 sl h^{-1} N_2 to maintain anaerobic conditions. Steady state conditions were examined after a minimum of three volume changes when biomass and acetate concentrations as well as gas uptake was constant. Samples were taken in regular intervals to measure OD_{600} and estimate biomass growth. The culture broth was centrifuged at 14,000 rpm (21,913 g) for 5 min and the supernatant was used for HPLC analysis of acetate and formate.

2.6. Biomass determination

Biomass concentrations were determined gravimetrically by transferring 5 ml of cultivation broth into pre-weighed glass tubes. The tubes were centrifuged at 4,800 rpm (2,396 g) for 10 min, washed with 5 ml of distilled water and centrifuged again. The biomass was dried for at least 72 h at 105 °C. Gravimetric biomass determination was carried out at the end of the batch phase and at the cultivation end. The optical density at 600 nm (OD_{600}) was measured in a spectrophotometer (Genesys™ 20, Thermo Fisher Scientific, Waltham, MA, USA) against a water blank. Gravimetrically determined biomass concentrations were correlated with OD_{600} values (biomass = 0.43 * OD_{600}) and this correlation was used to estimate the biomass concentration for all other time points.

2.7. HPLC analysis

Substrates and products in the liquid medium were determined with an Aminex HPX-87H column (300 × 7.8 mm, Bio-Rad, Hercules/CA, USA) using an Ultimate 3000 system (Thermo Scientific, Waltham/MA, USA). 4 mM H_2SO_4 was used as a mobile phase and the column was operated at 60 °C at a flow rate of 0.6 ml min^{-1} for 30 min. 10 μl sample were injected onto the column (Erian et al., 2018). Detection was performed using a refractive index (Refractomax 520, Thermo Fisher Scientific, Waltham/MA, USA) and a diode array detector (Ultimate 3000, Thermo Fisher Scientific, Waltham/MA, USA). Chromeleon 7.2.6 Chromatography Data System (Thermo Fisher Scientific, Waltham/MA, USA) was used for control, monitoring and evaluation of the analysis. 450 μl of culture supernatant were mixed with 50 μl of 40 mM H_2SO_4

and centrifuged for 5 min at 14,000 rpm (21,913 g) at 4 °C. The remaining supernatant was used for further analysis. Standards at defined concentrations of formate, acetate, ethanol and fructose were treated the same way. A 5-point-calibration was used for quantification.

2.8. GC analysis

The concentrations of H_2, CO_2 and CO were determined using a gas chromatograph (Trace Ultra GC, Thermo Fisher Scientific, Waltham/MA, USA). 100 µl of sample were injected at 100 °C with a split ratio of 20 on a ShinCarbon ST 100/120 packed column (Restek Corporation, Bellefonte/PA, USA). The oven was kept at 30 °C for 6.5 min, temperature was increased by 20 °C min^{-1} to 250 °C and kept constant for 1.5 min. Argon 5.0 (Messer Austria GmbH, Gumpoldskirchen, Austria) was used as a carrier gas at a flow rate of 2 ml min^{-1}. Samples were analyzed with a thermal conductivity detector. The filament temperature, cell block temperature and transfer temperature were set to 370 °C, 240 °C and 200 °C, respectively. The combination of two electrical valves enabled offgas measurement of each of the four reactors in 2-hour intervals. Chromeleon 7.2.10 Chromatography Data System (Thermo Scientific, Waltham/MA, USA) was used for control, monitoring and evaluation of the analysis. The gas composition of each gas was determined before and after its use in the fermentation process and gas uptake rates were determined by calculating the difference to these reference gas concentrations.

2.9. Rate calculations and elemental balancing

In batch experiments, volumetric acetate production rates r_{Ace} [mmol $l^{-1}h^{-1}$] were calculated for every sampling point according to the equation:

$$r_{Ace} = \frac{c_{Ace,t} - c_{Ace,(t-1)}}{\Delta t} \quad [1]$$

where c_{Ace} represents the acetate concentration [mmol l^{-1}] at each time point and Δt the time difference [h] between measurements. Specific production rates q_{Ace} [mmol $g^{-1}h^{-1}$] were calculated according to:

$$q_{Ace} = \mu \frac{c_{Ace,t} - c_{Ace,(t-1)}}{c_{BM,t} - c_{BM,(t-1)}} \quad [2]$$

where c_{BM} represents the biomass concentration [g l^{-1}] at each time point and µ the specific growth rate [h^{-1}].The highest value of these uptake rates calculated between individual sampling points is described as the maximum production rate. Total volumetric acetate production rates were calculated by considering the final acetate concentration after the fermentation and the total process time.

The volumetric gas uptake rates HUR, COUR, and CO_2UR [mmol $l^{-1}h^{-1}$] were calculated after normalization of the gas composition using N_2 as inert gas. For the calculation of CO_2UR during continuous cultivations, the amounts of CO_2 and HCO_3^- accounting for saturation of fresh medium were considered using the solubility of CO_2, the Henderson-Hasselbalch equation assuming a pK_s of 6.2 and the feeding rate. The specific gas uptake rates q_{H2}, q_{CO} and q_{CO2} were obtained by dividing HUR, COUR and CO_2UR [mmol $g^{-1}h^{-1}$] by the biomass concentration.

In chemostats, r_{Ace} was calculated by multiplying the average acetate concentration from at least 3 data points from steady state conditions by the liquid dilution rate D. Specific rates for gas uptake and acetate production were obtained by dividing the volumetric rate by the average biomass concentration of steady state data points.

For elemental balancing, biomass was assumed to contain 50% (w/w) carbon and 0.6% (w/w) hydrogen. The degree of reduction (DoR) of biomass was assumed to be 4.15 mol electrons per mol of carbon (Rittmann et al., 2012). For hydrogen balancing, water production was assumed to correlate to substrate uptake with 0.5 mol water produced per mol hydrogen taken up, 0.5 mol water per mol formate and 1 mol water per mol CO (Bertsch and Müller, 2015b; Schuchmann and Müller, 2014). The influence of water formation can be neglected for the calculation of DoR balances. All balances closed well without consideration of yeast extract.

2.10. Metabolic modeling and flux balance analysis

To model intracellular fluxes, we adapted a previously published *A. woodii* core model (Koch et al., 2019) consisting of 118 reactions. The model considers energy conservation and redox balancing as previously described for *A. woodii* (Schuchmann and Müller, 2014). The biomass composition was assumed to be similar to *C. autoethanogenum* (Valgepea et al., 2017).

Flux balance analysis (FBA) was done using the *CellNetAnalyzer* toolbox (Klamt et al., 2007; von Kamp et al., 2017). For all simulations, the measured specific rates for biomass formation, substrate uptake rates (CO, CO_2, H_2) and acetate were used to constrain the model. These measurements bear redundancies with respect to carbon and redox balances in the metabolic model and, therefore, fluxes had to be corrected prior to the actual FBA calculations to obtain a consistent system. This was done by minimizing the relative changes in the measured rates necessary to obtain a consistent flux scenario ("Check feasibility" function in *CellNetAnalyzer*). FBA requires the formulation of an objective function and most FBA studies use maximization of biomass synthesis. Since the growth rate was fixed to the experimentally observed value, the pseudo reaction that quantifies the non-growth associated ATP maintenance (NGAM) demand was maximized instead. In this way, an upper bound of ATP available for NGAM processes was obtained.

3. Results and discussion

3.1. Gas composition

Industrial BFG typically contains high amounts of N_2, ~ 20% CO and CO_2, and ~ 3% H_2 (Hou et al., 2011). To determine the exact composition, the gas was filled into gas cylinders at the stack of the steel production site and analyzed for its main components (Table 1). The gas composition of the gas did not differ greatly from literature data (Hou et al., 2011; Molitor et al., 2016).

Some components of the BFG, especially high concentrations of CO, might inhibit growth of *A. woodii*. Growth was not possible on BFG alone (Fig. 2b), which confirmed that in contrast to other organisms, utilization of CO as the sole carbon and energy source is not possible in *A. woodii* (Bertsch and Müller, 2015b). The hypothesis was that blending BFG with H_2 would enable growth, acetate formation and CO_2 fixation in the CO-containing gas. To this end, two H_2 blending ratios were chosen: low (30%) and high (60%) H_2. In accordance, CO and CO_2

Table 1
Composition of gases used in this study. Low and high H_2 gases were blended with 30% H_2 and 60% H_2, respectively. n.d. = not determined; errors for CO_2, H_2 and CO determination in gas mixtures are 2% relative.

Blast furnace gas from industrial steel production site						
Gas composition [%]	N_2	CO_2	CO	H_2		
	48.5	22.7	25.2	3.6		
Gas blends used in this study						
Gas composition [%]	Calculated value			Actual value		
	CO_2	H_2	CO	CO_2	H_2	CO
Idealized, low H_2	16.5	30.0	–	16.6	30.3	–
Idealized, high H_2	9.4	60.0	–	9.6	60.0	–
Idealized with CO, low H_2	16.5	30.0	18.3	16.7	29.7	18.6
Idealized with CO, high H_2	9.4	60.0	10.4	9.5	60.1	10.6
BFG, low H_2*	16.5	30.0	18.3	n.d.	n.d.	n.d.
BFG, high H_2*	9.4	60.0	10.4	8.8	62.2	9.8
Standard	20.0	80.0	–	20.0	80.0	–

partial pressures were higher in the low H_2 blend compared to the high H_2 blend. To investigate the effect of the presence of CO as well as other potential inhibitors in the industrial flue gas, performance of *A. woodii* was additionally investigated using idealized gases. Concentrations of CO, CO_2 and H_2 in idealized gases were identical to those in BFG blended with the same amount of H_2. In one approach, the gas only consisted of CO_2, N_2 and H_2, which allowed to determine effects mediated by the presence of CO. In another approach, CO, CO_2, N_2 and H_2 were present and the effect of other potential inhibitors could be studied. Table 1 gives an overview of all gas compositions used in this study.

3.2. Utilization of blast furnace gas requires adaptation phase

In a first step, the utilization of different gases by *A. woodii* was tested in serum bottle experiments. Growth and acetate production were compared using idealized gas and BFG at the low and high H_2 blend. Performance was also monitored for a standard gas composition of 20% CO_2 and 80% H_2.

While growth and acetate production started immediately on idealized and standard gas blends, the culture containing CO displayed a lag phase of ~ 100 h (Fig. 1a and 1c). This adaptation phase could be reduced by transferring cells from a culture growing on CO-containing BFG (stage 1) to fresh medium (stage 2, Fig. 1b and 1d). This observation implies that *A. woodii* can be adapted to growth on BFG by sequential transfers. Maximum acetate production rates were similar in both cultivations, but the total volumetric acetate productivity was increased in stage 2 cultivations due to the reduction of the adaptation phase (Table 2). An adaptation phase of *A. woodii* grown on CO has previously been described and the delay was hypothesized to be a result of the time required for expression of enzymes involved in CO metabolism (Bertsch and Müller, 2015b). Conclusively, the efficient utilization of BFG is possible in *A. woodii* when cells have previously been adapted to growth on CO-containing gas.

3.3. Formate addition reduces adaptation phase during growth on CO

CO toxicity in acetogens is caused by an inhibitory effect on hydrogenases, i.e. the hydrogen dependent CO_2 reductase (HDCR). The methyl branch of the WLP can alternatively be fed with formate instead of CO_2 and H_2, which finally allows for growth and CO utilization (Bertsch and Müller, 2015b). To investigate whether the addition of formate can improve growth and production characteristics on BFG, further experiments were carried out in serum bottles. BFG alone and the high H_2 blend BFG were used as carbon and energy source and cultures with and without formate were compared (Fig. 2).

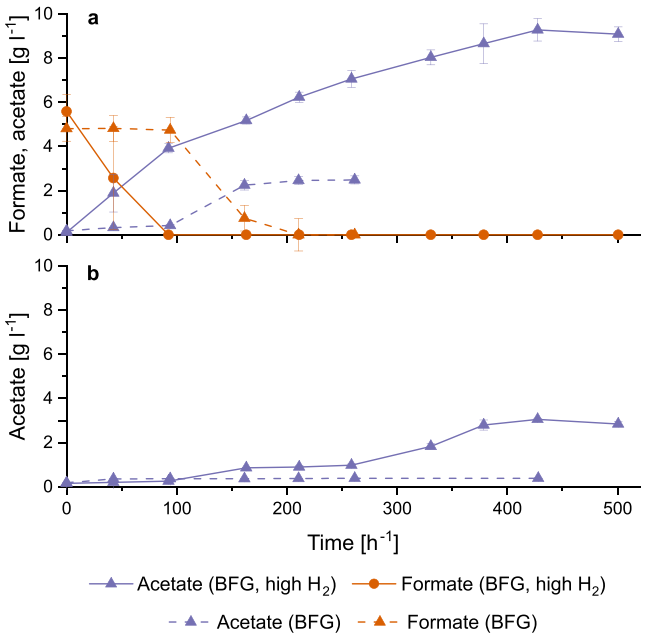

Fig. 2. Addition of formate circumvents adaptation phase of *A. woodii* during growth on CO-containing gas. Growth on industrial furnace gas with 60% H_2 in phosphate-buffered medium is compared with (a) or without (b) the addition of 5 g l^{-1} formate. Results represent means and standard deviations from biological duplicates in serum bottle experiments.

While cultivations without formate displayed a growth delay of ~ 150 h, no lag phase was observed when cultures were provided with formate. Growth and acetate production even continued in BFG with H_2 after formate was depleted, indicating co-consumption of CO, CO_2 and

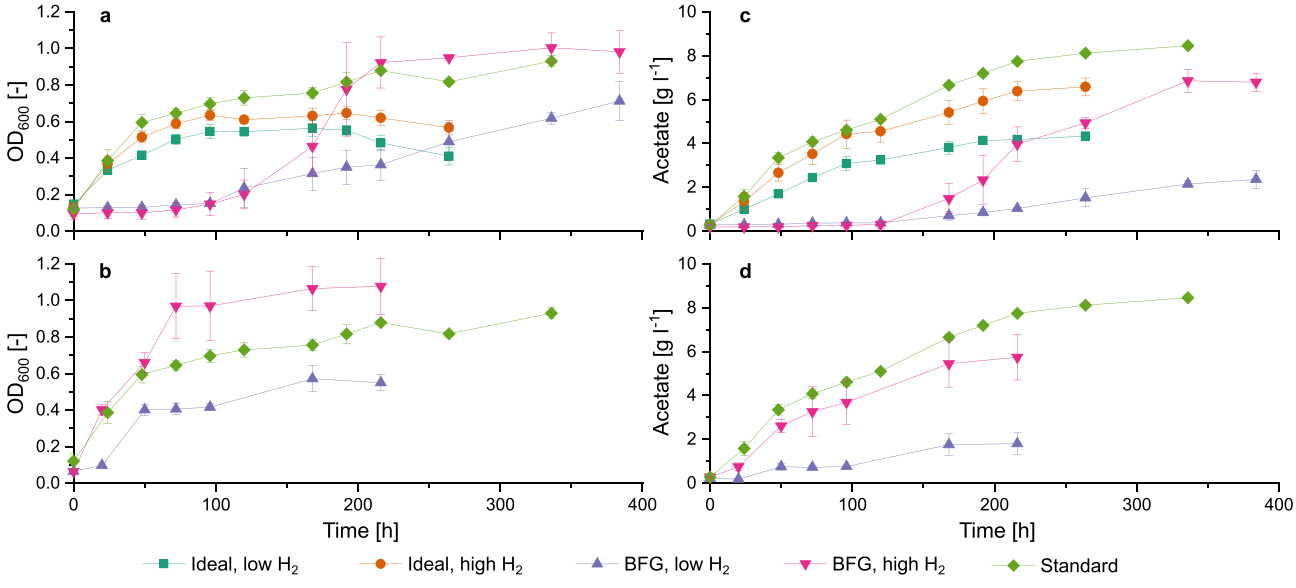

Fig. 1. Adaptation prevents growth delay in *A. woodii* during growth on CO containing gas. Industrial furnace gas (real) diluted with H_2 was compared to idealized gas without CO and a standard mixture (80% H_2, 20% CO_2). a and b inoculation from mixotrophically growing cells (Stage 1), c and d inoculation with adapted cells from the first stage (Stage 2). Bicarbonate-buffered medium was used. Results represent means and standard deviations from biological triplicates in serum bottle experiments.

Table 2
Maximum and total acetate productivity of *A. woodii* on gases of different compositions. Means and standard deviations of biological triplicates are shown in bicarbonate-buffered medium. After growth on CO-containing gas (stage 1), adapted cells were transferred to fresh medium (stage 2).

Gas blend	CO_2 [%]	H_2 [%]	CO [%]	$r_{Ace, max}$ [mmol $l^{-1}h^{-1}$]	$r_{Ace, total}$ [mmol $l^{-1}h^{-1}$]
Idealized, low H_2	16.7	30.0	–	12.2 ± 0.1	7.9 ± 0.1
Idealized, high H_2	9.5	60.0	–	21.8 ± 0.9	11.3 ± 0.9
BFG, low H_2, stage 1	16.7	30.0	18.5	4.1 ± 0.5	2.2 ± 0.5
BFG, high H_2, stage 1	9.5	60.0	10.6	27.2 ± 0.6	7.9 ± 0.6
BFG, low H_2, stage 2	16.7	30.0	18.5	7.6 ± 0.5	3.7 ± 1.0
BFG, high H_2, stage 2	9.5	60.0	10.6	24.7 ± 5.7	12.3 ± 2.5
Standard	20.0	80.0	–	29.3 ± 0.2	13.8 ± 0.2

H_2. When CO was present as the sole carbon and energy source, acetate production ceased after formate depletion (Fig. 2a). More acetate was produced in experiments where formate was added, potentially due to a pH stabilizing effect of formate. Acetate titers in the experiment without formate are not comparable to initial experiments since phosphate-buffered instead of bicarbonate-buffered medium was used. Apart from differences in buffer capacities, the presence of bicarbonate potentially also influenced enzymes of the WLP or enzymes involved in energy conservation, as shown for *Thermoanaerobacter kivui* (Schwarz et al., 2020; Schwarz and Müller, 2020). Conclusively, the addition of formate to cultures of *A. woodii* containing CO in the gas phase reduced the lag-phase and enabled growth on BFG blended with H_2 after formate depletion.

3.4. Batch cultivations show feasibility of CO, CO_2 and H_2 co-utilization

In contrast to experiments in serum bottles, continuously supplied gas in bioreactor cultivations enhances substrate availability and improves productivity. To study whether growth of *A. woodii* on CO-containing BFG is also feasible in bioreactor cultivations and to investigate acetate production and uptake characteristics of the individual gases, batch experiments were carried out. Since high H_2 blends were shown to result in superior production characteristics, this blend was chosen for cultivations with idealized gas with and without CO. Formate was added in cultivations using CO-containing gas to facilitate efficient growth.

During growth on gas with only CO_2 and H_2, uptake rates of these two gases approximately represented a stoichiometric ratio of 2:1 (Fig. 3a and 3b). Gas uptake rates increased steadily until reaching their maximum after 50 – 60 h. High and inhibitory acetate concentrations in the culture broth might have been a reason for the subsequent decrease of gas uptake. Although biomass formation ceased in the late batch phase, acetate was still produced.

When CO was present in the gas, it was first co-utilized with formate, resulting in the production of CO_2 and H_2 (Fig. 3c and 3d). As soon as CO in the offgas dropped below 8.5% CO (from the initial 10.6%), CO_2 and H_2 uptake started. Subsequently, CO, CO_2 and H_2 co-utilization progressed and continued even after the depletion of formate. In accordance with cultivations on idealized gas without CO, the uptake rates of CO_2 and H_2 decreased after ~ 50 h of cultivation. Product inhibition by high acetate concentrations could have been responsible for these decreasing gas uptake rates. While inhibition by acetate has been described to occur between 8 and 12 g l^{-1} acetate (Kantzow et al., 2015), in this study impaired gas uptake rates were only observed when acetate titers exceeded 20 g l^{-1}.

The final biomass concentration was 3-fold higher in cultivations on gas containing CO, whereas the final acetate titer was increased by 16% (Table 3). Data from bioreactor cultivations therefore confirmed the previous observation that the utilization of CO is beneficial for biomass formation in *A. woodii* due to a 5-fold higher ATP yield (Bertsch and Müller, 2015a,b). Volumetric H_2 uptake rates were comparable in both cultivations, which suggests a limitation during the exponential growth phase. Increased biomass concentrations during cultivation on CO, CO_2 and H_2 in combination with comparable H_2 uptake rates generally resulted in decreased specific uptake rates on CO-containing gas.

The maximum specific growth rate (μ_{max}) was ~ 0.1 h^{-1} on both gases (Table 3) and is comparable to values previously reported (0.112 h^{-1} and 0.125 h^{-1} on H_2/CO_2 and formate-CO, respectively) (Bertsch and Müller, 2015b).

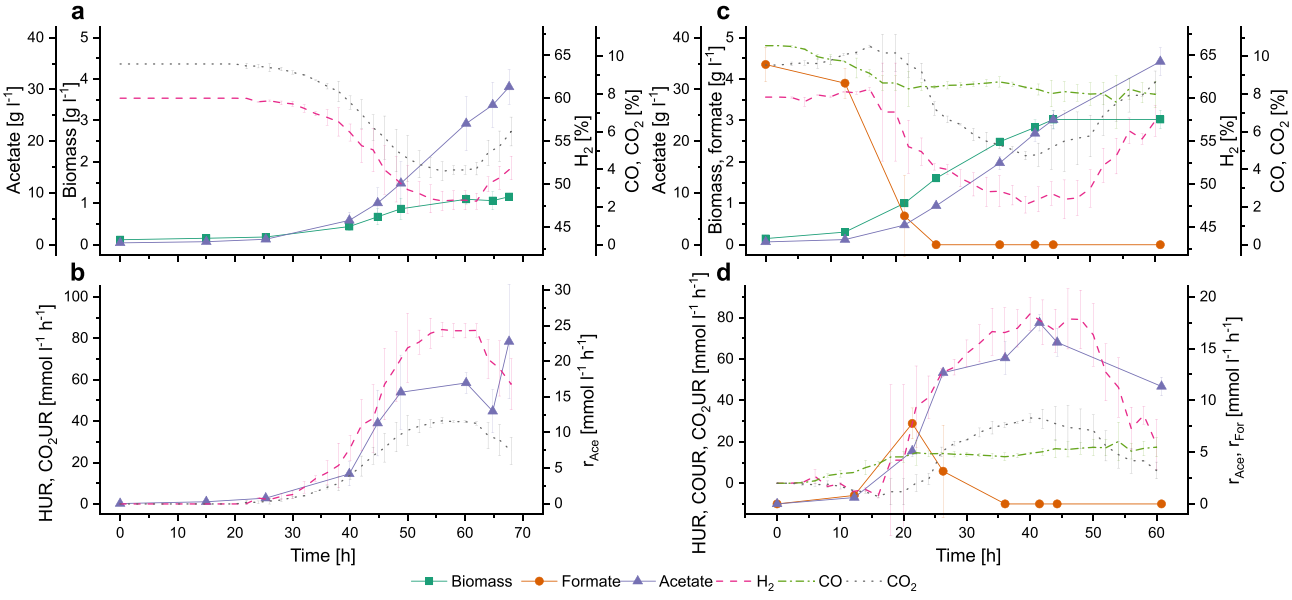

Fig. 3. Growth and acetate production in batch cultivations of *A. woodii* on idealized gas blends. Idealized gas without CO (a, b) and with CO (c, d) with 60% H_2 were compared. The gas composition (in %) in a and c is based on the gas flow rate of the ingas. Results represent mean values and standard deviations from biological duplicates of bioreactor cultivations.

Table 3
Fermentation characteristics of *A. woodii* cultivations in batches on idealized gas mixtures containing 60% H_2 with and without CO. Maximum volumetric and specific production (acetate) and uptake (H_2, CO_2 and CO) rates are shown. Means and standard deviations were calculated from biological duplicates.

Gas blend	Titer [g l^{-1}]		Max. spec. growth rate [h^{-1}]	Maximum volumetric rates [mmol $l^{-1}h^{-1}$]				Maximum specific rates [mmol $g^{-1}h^{-1}$]				Balance [%]		
	Acetate	Biomass	μ_{max}	r_{Ace}	HUR	CO_2UR	COUR	q_{Ace}	q_{H2}	q_{CO2}	q_{CO}	Carbon	Hydrogen	DoR
Idealized without CO, high H_2	30.5 ± 3.3	1.16 ± 0.08	0.10 ± 0.03	22.8 ± 8.0	84.1 ± 4.2	40.3 ± 0.4	–	21.1 ± 2.0	82.9 ± 4.8	39.6 ± 0.3	–	112 ± 16	108 ± 3	108 ± 6
Idealized with CO, high H_2	35.4 ± 2.7	3.02 ± 0.22	0.13 ± 0.01	17.5 ± 0.8	79.8 ± 13.8	31.2 ± 4.6	19.8 ± 1.3	9.9 ± 0.4	41.0 ± 13.5	17.5 ± 1.9	11.8 ± 1.3	87 ± 1	101 ± 7	82 ± 6

3.5. Continuous cultivations are limited in gas liquid mass transfer of H_2

After demonstrating simultaneous CO, CO_2 and H_2 uptake in batch cultivations, this study aimed to characterize gas uptake, growth, and acetate formation under steady state conditions in continuous cultivations of *A. woodii*. Therefore, gas-limited cultures were established as a basis for solid characterization of the process performance. To study H_2 limitation, the influence of different H_2 partial pressures and gas-liquid mass transfer rates were first investigated independently from the presence of CO. Chemostats were performed on low (30%) and high (60%) H_2 blend idealized gas (without CO) at a dilution rate of 0.05 h^{-1} (~50% of μ_{max}).

Acetate was produced at a rate of 15.6 mmol $l^{-1}h^{-1}$ at 600 rpm in the high H_2 blend, which is ~ 20% higher compared to the low H_2 blend and 60% of the rates observed in batch experiments. H_2 and CO_2 uptake rates were enhanced by 20% due to the improved availability of H_2 in the high H_2 blend. Gas transfer is typically proportional to partial pressures and several factors can influence hydrogen solubility (Demler and Weuster-Botz, 2011). Apart from media additives like e.g. antifoam, increased biomass concentrations were reported to decrease H_2 solubility (Cotter et al., 2009). Subsequently, it was examined whether cultivations at 600 rpm were limited in H_2 gas-liquid mass transfer by increasing and decreasing the stirrer speed to 1200 and 300 rpm, respectively.

Increasing the stirrer speed from 600 rpm to 1200 rpm improved gas–liquid mass transfer as indicated by enhanced gas uptake rates (Fig. 4). In both approaches at the high and low H_2 blend, the enhanced volumetric power input increased volumetric H_2 uptake and acetate production rates to 150%, while specific uptake rates stagnated or increased by 30% in the high and low H_2 blend, respectively (Table 4). A decrease of the stirrer speed from 600 rpm to 300 rpm drastically reduced H_2 uptake and acetate production to ~ 20%. Therefore, cultures were indeed H_2-limited at a stirrer speed of 600 rpm.

In addition to a limitation of the H_2 gas-liquid mass transfer, continuous cultivations on H_2 and CO_2, could be limited by the following mechanisms: (i) limitation in the liquid medium, e.g. nitrogen source or a trace element, (ii) CO_2 limitation, (iii) a physiological limitation, i.e. by reaching maximum uptake or production per cell or (iv) product inhibition. To exclude any other limitation the other four limitation possibilities were systematically examined. The cultivation performance was not restrained by neither yeast extract nor trace elements, since individual pulses of these components at steady state conditions showed no effect on gas uptake rates, biomass, or acetate production (data not shown). A limitation in gas-liquid transfer of CO_2 is not probable, because the CO_2 transfer rate is still 4.5-fold higher than the H_2 transfer rate under the conditions tested (pH_2 = 60%, pCO_2 ~ 10%). Since the acetate concentration as well as the specific H_2 uptake and acetate production rates were higher at 1200 compared to 600 rpm, a physiological limitation or product inhibition is also unlikely.

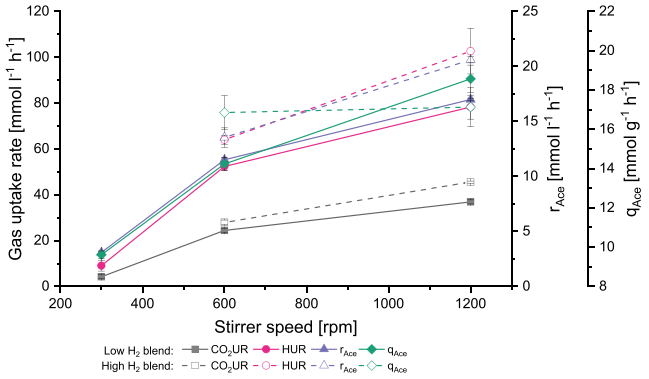

Fig. 4. Increased gas liquid mass transfer improves growth of *A. woodii* on CO_2 and H_2. Mass transfer was improved by increasing stirrer speed. Results represent means and standard deviations of biological duplicates in steady state during continuous cultivation.

Production rates obtained in chemostat experiments (13.5 mmol $l^{-1}h^{-1}$) are within 7% to previous reports, where a slightly lower acetate productivity of 12.6 mmol $l^{-1}h^{-1}$ (=302.4 mmol l^{-1} d^{-1} = 18.2 g l^{-1} d^{-1}) was observed during continuous cultivations of *A. woodii* (Kantzow et al., 2015). There, acetate productivity but not acetate concentration was increased in a cultivation system with cell retention. In contrast to this study, H_2 uptake rates were not comparable in batch and chemostat experiments. Concomitantly, acetate concentrations reached ~ 22 g l^{-1} in continuous cultivations (Kantzow et al., 2015). Since product inhibition was observed at acetate concentrations above 20 g l^{-1} in batch experiments of this study, it is possible that continuous cultivations described by Kantzow et al. (2015) were limited by product inhibition rather than by H_2 transfer. When aiming for gas-limited processes, the focus should therefore be laid on achieving acetate concentrations below 20 g l^{-1}. Conclusively, it was shown that autotrophic cultivations with *A. woodii* on H_2 and CO_2 are very flexible regarding the gas composition and gas-liquid mass transfer. Cultivations at 600 rpm at low and high H_2 blend were limited in H_2 availability, which makes these conditions suitable for further process characterization.

3.6. Dynamic gas–liquid mass transfer shifts allow to approximate maximum q_{H2}

To determine the physiological limit of the gas fermentation system, this study aimed to approximate the maximum possible specific H_2 uptake rate. This important characteristic of the host strain can contribute to a better understanding of the physiology of *A. woodii* and facilitate further process development. To this end, a dynamic experiment with a shift from lower to higher volumetric power input and thus from lower to higher hydrogen transfer rate was performed. At low biomass concentrations, *A. woodii* cannot utilize all available H_2 and will grow at maximum q_{H2} until cells are no longer physiologically limited. Since uptake rates of H_2 and CO_2 as well as acetate are stoichiometrically dependent (H_2 : CO_2 ~ 2:1, H_2 : acetate ~ 4:1), different approaches can be used to approximate the maximum q_{H2}: directly via online measurement of HUR or indirectly via online measurement of CO_2 and offline determination of acetate.

Table 4
Steady state data of *A. woodii* chemostat cultivations on idealized gas mixtures without CO under varying mass transfer. Means and standard deviations were calculated from biological duplicates. DoR = degree of reduction.

Idealized without CO	Stirrer speed [rpm]	Titer [g l^{-1}]		Volumetric rates [mmol l^{-1} h^{-1}]			Specific rates [mmol $g^{-1}h^{-1}$]			Yields [mol mol^{-1}]		Balance [%]		
		Biomass	Acetate	r_{Ace}	HUR	CO_2UR	q_{Ace}	q_{H2}	q_{CO2}	$Y_{Ace/CO2}$	$Y_{Ace/H2}$	Carbon	Hydrogen	DoR
Low H_2 blend	300	0.32 ± 0.02	3.7 ± 0.3	3.1 ± 0.1	9.0 ± 2.4	4.2 ± 1.6	9.6 ± 0.2	27.9 ± 9.6	12.3 ± 4.8	0.67 ± 0.29	0.36 ± 0.10	123 ± 35	104 ± 17	114 ± 36
	600	0.82 ± 0.02	13.3 ± 0.91	11.5 ± 0.2	52.3 ± 1.7	24.3 ± 0.9	14.2 ± 0.3	64.6 ± 1.3	30.1 ± 0.8	0.47 ± 0.02	0.22 ± 0.01	103 ± 4	99 ± 9	95 ± 4
	1200	0.92 ± 0.03	17.2 ± 0.1	17.0 ± 0.1	78.2 ± 5.2	36.3 ± 0.8	18.6 ± 0.7	85.6 ± 8.5	39.7 ± 3.1	0.47 ± 0.02	0.22 ± 0.01	100 ± 5	94 ± 3	93 ± 7
High H_2 blend	600	0.80 ± 0.01	15.6 ± 0.2	13.5 ± 0.9	64.0 ± 2.0	28.6 ± 1.0	16.9 ± 0.9	79.7 ± 1.2	35.6 ± 1.8	0.48 ± 0.05	0.21 ± 0.01	102 ± 10	93 ± 1	90 ± 3
	1200	1.20 ± 0.05	19.5 ± 0.2	20.6 ± 0.2	102 ± 10	46.2 ± 0.5	17.1 ± 1	85.2 ± 4.5	38.4 ± 2.1	0.45 ± 0.01	0.20 ± 0.02	96 ± 1	91 ± 5	87 ± 10

After an increase of the stirrer speed at 280.2 h, specific H_2 and CO_2 uptake instantly increased, remained constant for ~ 20 h and subsequently decreased (Fig. 5a). To correct for errors and variations in quantification of specific uptake rates, the volumetric rates were plotted over the biomass concentration during growth at maximum q_{H2} (Fig. 5b). Data was fitted by linear regression, where the slope represents the corresponding maximum specific rate. These fitted specific rates indicate that the maximum specific H_2 uptake rate $q_{H2,max}$ is between 116 and 167 mmol $g^{-1}h^{-1}$ (Table 5). By setting the gas uptake rate to 0 mmol $l^{-1}h^{-1}$ and solving the linear regression for the biomass concentration (X), the result represents the amount of biomass produced at no gas uptake. This biomass production can be attributed to the presence of yeast extract in the medium and was used to correct carbon balances of chemostat cultivations at low gas transfer rates (300 rpm). An approximation of the acetate production from yeast extract was performed accordingly.

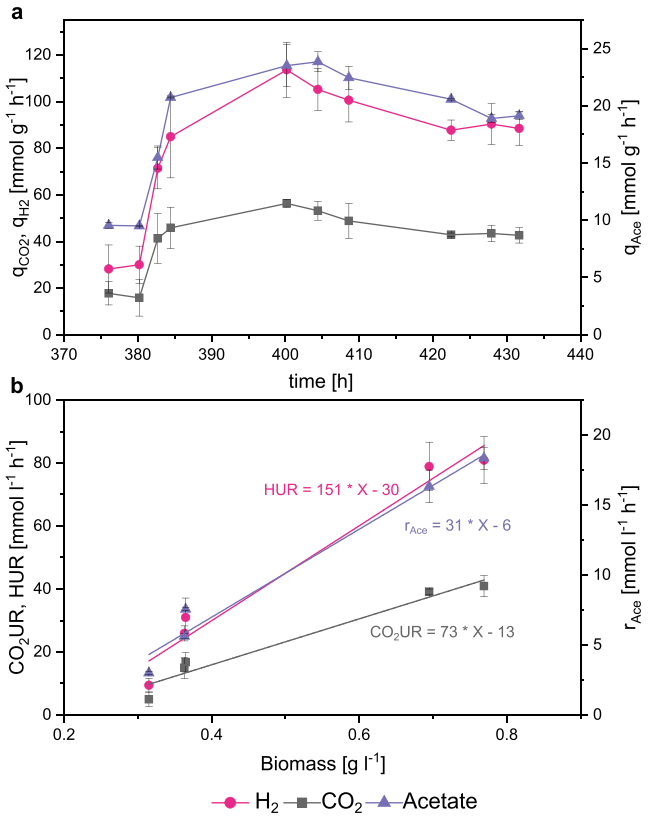

Fig. 5. Approximation of maximum q_{H2} using dynamic shift experiments of *A. woodii* on CO_2 and H_2. a, specific uptake and production rates. Cultivation was shifted from low mass transfer (300 rpm) to high mass transfer (1200 rpm) at 380.2 h. b, volumetric CO_2 and H_2 uptake and acetate production from 380.2 h to 440.4 h (linear range). The data was fitted by linear regression (X = biomass). The slope represents the maximum specific rate and when X is set to zero, the biomass concentration at no gas uptake (and thus only from yeast extract in the medium) can be obtained. Results represent means and standard deviations of biological duplicates during continuous cultivation.

Comparing the approximated $q_{H2,max}$ to steady state data on idealized gas revealed that all specific rates obtained at steady state conditions were lower than the possible maximum. Therefore, a physiological limitation of *A. woodii* in any chemostat cultivation in this study is unlikely.

3.7. *A. woodii* can efficiently utilize CO_2 in gases containing CO

After characterizing growth of *A. woodii* on CO_2 and H_2 containing gases, CO, CO_2 and H_2 utilization in BFG was studied and the effects of CO on *A. woodii* metabolism was determined. To this end, continuous cultivations were compared using idealized gas with CO at low and high H_2 blends and BFG at high H_2 blend.

The transition from batch to continuous cultures was found to be crucial for successful growth on CO-containing gas. The optimal starting point for the continuous cultivation was after formate had been depleted, but when CO, CO_2 and H_2 were still co-utilized and before CO_2 and H_2 uptake decreased at the end of the batch. Since formate was not added to the feed, all cultivations on CO-containing gas were carried out autotrophically similar to chemostats without CO.

A. woodii was able to co-utilize CO, CO_2 and H_2 in all gas compositions and even at higher CO partial pressures (low H_2 blend, Table 6). A comparison of steady state data confirmed observations from batch experiments, where biomass increased with increasing CO partial pressure (decreasing pH_2). Higher CO partial pressures decreased acetate titers, which was also reflected by the higher specific acetate productivity in

Table 5
Process characteristics of *A. woodii* obtained from mass transfer shift experiment. To increase gas transfer into the liquid phase, stirrer speed was increased from 300 to 1200 rpm. Data was obtained from linear regression of volumetric rates with biomass concentrations. Means and standard error of regression are shown.

Calculation for	Slope = specific gas uptake rate [mmol $g^{-1}h^{-1}$]	R^2	$q_{H2,\ max}$ [mmol $g^{-1}h^{-1}$]	Intercept [mmol $l^{-1}h^{-1}$]	Biomass at no gas uptake [g l^{-1}]
H_2	151 ± 16	0.966	151 ± 16	−30.4 ± 8.7	0.20 ± 0.08
CO_2	73 ± 9	0.957	146 ± 18	−13.3 ± 4.8	0.18 ± 0.09
Acetate	32 ± 3	0.974	128 ± 12	−5.6 ± 1.6	–

Table 6
Steady state data of *A. woodii* chemostat cultivations on gas mixtures containing CO. Stirrer speed was set to 600 rpm. Means and standard deviations were calculated from biological duplicates DoR = degree of reduction.

Gas blend	Titer [g l^{-1}]		Volumetric rates [mmol $l\ h^{-1}$]				Specific rates [mmol $g^{-1}h^{-1}$]				Yields [mol mol^{-1}]		Balance [%]		
	Biomass	Acetate	r_{Ace}	HUR	COUR	CO_2UR	q_{Ace}	q_{H2}	q_{CO}	q_{CO2}	$Y_{Ace/CO2}$	$Y_{Ace/H2}$	Carbon	Hydrogen	DoR
Idealized with CO, low H_2 blend	1.86 ± 0.07	13.4 ± 0.7	12.6 ± 0.7	40.8 ± 2.5	22.1 ± 0.9	10.6 ± 0.2	6.8 ± 0.6	21.9 ± 0.6	11.9 ± 0.4	5.5 ± 0.1	0.37 ± 0.01	0.29 ± 0.01	89 ± 3	86 ± 6	95 ± 8
Idealized with CO, high H_2 blend	1.54 ± 0.12	17.8 ± 1.5	16.6 ± 0.7	71.6 ± 2.3	13.4 ± 1.4	26.2 ± 0.2	10.8 ± 0.4	46.6 ± 2.2	8.7 ± 0.2	17.1 ± 1.2	0.43 ± 0.01	0.23 ± 0.01	93 ± 1	87 ± 1	87 ± 1
BFG, high H_2 blend	1.27 ± 0.06	15.1 ± 0.7	14.3 ± 0.4	72.2 ± 8.0	12.5 ± 8.1	20.8 ± 5.7	11.1 ± 0.8	51.2 ± 13.0	9.5 ± 6.3	16.1 ± 5.5	0.44 ± 0.04	0.23 ± 0.05	97 ± 8	86 ± 1	81 ± 3

the high H_2 blend compared to the low H_2 blend. Uptake rates of CO, CO_2 and H_2 differed for the low and high H_2 blend. While HUR was 1.8-fold higher in the high H_2 blend of idealized gas with CO, COUR was 1.7-fold lower. These ratios correspond to the differences in partial pressures of the two gases, suggesting that cultures were limited in CO and H_2. CO and H_2 limitation were also experimentally demonstrated as decreasing the stirrer speed from 600 rpm to 300 rpm resulted in decreased gas uptake rates (data not shown). Surprisingly, H_2 uptake rates were lower in high H_2 blends when gases did not contain CO (Table 4 and 6). Apart from the influence of biomass concentration on H_2 and CO solubility (Cotter et al., 2009; Rittmann et al., 2012), the presence of other gases could potentially influence gas uptake or solubility. Since H_2 was the limiting factor in all chemostats, the uptake of CO_2 was stoichiometrically coupled to H_2 utilization. Because CO was utilized as an additional carbon and energy source, total carbon turnover (i.e. CO and CO_2) was higher compared to gases without CO. Utilization of CO reduced CO_2 uptake, but still enabled net CO_2 fixation even in the low H_2 blend with a high partial pressure of CO.

Cultivations of *A. woodii* on industrial BFG resulted in similar gas uptake rates compared to idealized gas with CO and the same H_2 blending ratio. Biomass and acetate production were slightly decreased, and acetate productivity reached 86% of the rate on idealized gas of the same composition. The specific acetate productivity remained constant due to identical H_2 and CO partial pressures. The slight difference in production rates on real and idealized gas with CO indicates that other inhibitors in the BFG could have had a minor influence on the performance of *A. woodii*. Gas uptake rates during the cultivation on BFG varied to a greater extent than on idealized gas with CO. These variations can probably be attributed to the *in situ* blending of two independent gas streams, whereas premixed gases were used for all other bioreactor experiments. The fact that *A. woodii* was not negatively influenced by these fluctuations renders the organism suitable for industrial applications, since similar deviations of the gas composition might also occur in large-scale fermentations.

During growth on CO_2 and H_2 alone, specific H_2 uptake rates of *C. autoethanogenum* were ~ 60% of those in *A. woodii* (Heffernan et al., 2020). Based on the comparison of specific CO and H_2 uptake rates, the high efficiency of H_2 and CO_2 utilization by *A. woodii* compared to *C. autoethanogenum* and *C. ljungdahli* was therefore confirmed in this study (Hermann et al., 2020; Schuchmann and Müller, 2014; Takors et al., 2018). On the other hand, for gases with comparable CO and H_2 partial pressures, higher specific CO uptake rates were observed in *C. autoethanogenum*, while q_{H2} was only 60% of the maximum reached using BFG in this study (Valgepea et al., 2018).

The fact that CO utilization in *A. woodii* is less efficient compared to other acetogens has long been described. Potential reasons include that *A. woodii* is more affected by the inhibition of hydrogenases by CO compared to other acetogens because the organism reduces CO_2 directly with H_2 instead of redox equivalents (NAD(P)H and/or reduced ferredoxin) used by *C. autoethanogenum* and *C. ljungdahlii* (Bertsch and Müller, 2015a,b; Mock et al., 2015; Ragsdale and Ljungdahl, 1984; Schuchmann and Müller, 2014; Schwarz et al., 2020). In addition to hydrogenase inhibition, the efficiency of the CO dehydrogenase reaction has also been speculated to be responsible for efficient CO utilization (Liew et al., 2016a; Ragsdale et al., 1983). *T. kivui* could be adapted to growth on high concentrations of CO even though the organism also uses H_2 for CO_2 reduction to formate (Weghoff and Müller, 2016). Therefore, it was suggested that monofunctional CO dehydrogenases might play an important role in CO metabolism to quickly scavenge CO and prevent hydrogenase inhibition.

Fermentation of CO_2 and H_2 using *C. autoethanogenum* was found to be improved by adding small amounts of CO (Heffernan et al., 2020). While CO_2 and H_2 partial pressures were comparable to this study, CO concentrations in the gas were only 2%. In this study, net CO_2 fixation was achieved by simultaneous uptake of CO_2 and H_2 with CO at higher CO and lower H_2 concentrations of 18 and 30%, respectively. CO and H_2 partial pressures of 15 and 45%, respectively, comparable to this study promoted efficient CO utilization and a shift towards reduced metabolites in *C. autoethanogenum* but resulted in the production of small amounts of CO_2 (Valgepea et al., 2018).

Prior to this study, *A. woodii* had not been considered for fermentation of CO-rich industrial gases. Moreover, CO utilization at comparable gas compositions usually results in net CO_2 production (Hermann et al., 2020; Valgepea et al., 2018, 2017). Here, it was shown that *A. woodii* is highly flexible regarding co-utilization of CO, CO_2 and H_2 at different gas compositions allowing net CO_2 fixation. H_2 blending in combination with an efficient H_2 metabolism renders *A. woodii* a suitable host for CO_2 fixation from industrial gases even in the presence of CO.

3.8. Intracellular flux distributions depend on H_2 and CO availability

To model intracellular flux distributions, specific uptake and production rates from chemostat cultivations on idealized gas with and without CO were. An *A. woodii* core model was used for FBA simulations. In typical FBA studies, maximization of biomass synthesis is used as objective function. Since the growth rate was fixed to the experimentally observed value, the pseudo reaction that quantifies the non-growth associated ATP maintenance (NGAM) demand was maximized instead. In this way, an upper bound of ATP available for NGAM processes was obtained. Fig. 6 summarizes the simulation results for intracellular fluxes of the carbon, redox and energy metabolism. Experimental data of biomass formation as well as specific uptake (CO, CO_2 and H_2) and acetate excretion rates proved to be very consistent, since in all scenarios considered only small corrections for measured fluxes were necessary (Fig. 6). In terms of ATP production, the specific flux through the ATPase increased by ~ 20% for high H_2 compared to low H_2 for H_2/CO_2 fermentations. ATP generation was further increased in the presence of CO regardless of the H_2 partial pressure. In detail, low and high CO partial

pressures increased flux through the ATPase by an additional 20% compared to the corresponding H_2/CO_2 without CO. Likewise, the NGAM was lowest for the condition using low H_2 without CO (0.9 mmol $g^{-1}h^{-1}$) and highest for the high H_2 in combination with CO (2.4 mmol $g^{-1}h^{-1}$). Generally, higher maintenance ATP demands in the presence of high H_2 or CO could be a result of additional protein synthesis required. Furthermore, higher acetate concentrations were observed when high H_2 was used, which could also increase the ATP demand to maintain the proton gradient across the membrane.

Model simulations showed that at lower CO and high H_2 partial pressures (i.e. high H_2 blend), CO was only assimilated in the carbonyl branch, thus only serving as a carbon, but not as an electron source (Fig. 6b). Usually, CO serves as the main electron source during acetogenic growth on CO or syngas and CO_2 produced is only partially utilized in the methyl branch (Hermann et al., 2020; Valgepea et al., 2018, 2017), which in this study was the case at higher CO and lower H_2 partial pressures (i.e. low H_2 blend). CO was therefore used both as a carbon and electron source, which resulted in increased availability of reducing equivalents, i.e. reduced ferredoxin. This change in metabolic activity finally led to differences in co-factor distribution and energy conservation. In this study, net CO_2 fixation was achieved in gases at CO/H_2 ratios of 0.18 to 0.62. Based on the CO_2 uptake rates for these ratios, linear extrapolation would indicate that net CO_2 fixation would be possible up to a CO/H_2 ratio of 0.92 (linear regression of CO_2UR and CO/H_2 ratio). If the goal was to utilize CO_2 only via the methyl and CO only via the carbonyl branch and the flux through CO dehydrogenase linearly correlated with CO partial pressures, the BFG would have to be blended with 44% H_2 (linear regression of CODH flux and pCO). In other words, blending industrial BFG with H_2 as an energy source can be used to control individual gas uptake rates and shift *A. woodii* metabolism

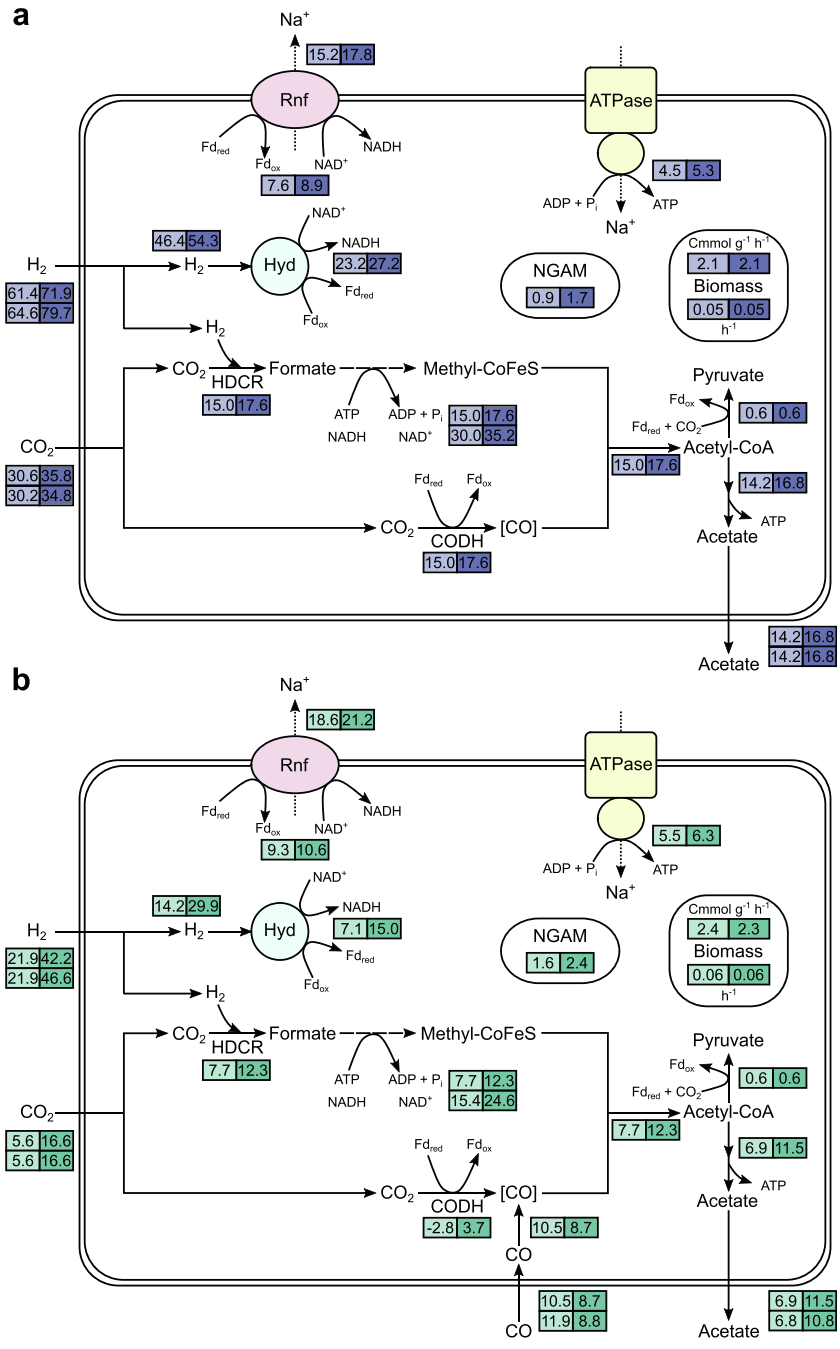

Fig. 6. Metabolic flux distributions of *A. woodii* chemostat cultivations depend on gas composition. Flux distributions for a, idealized gas without CO with low H_2 (30%) (light blue) and high H_2 (60%) (dark blue) and b, idealized gas with CO with low H_2 (30%) (light green) and high H_2 (60%) (dark green). Experimentally determined specific rates were used as input data and constraints for FBA simulations with maximization of the ATP maintenance pseudo reaction (NGAM) as the objective function. All fluxes are shown in mmol $g^{-1}h^{-1}$ (Biomass box: upper values in Cmmol $g^{-1}h^{-1}$, lower values in h^{-1}) and represent means of biological duplicates. Upper values for uptake and production rates represent experimental data, lower values represent data used for FBA simulation. Model input values may slightly deviate from measured experimental data because stoichiometric inconsistencies were corrected (see Methods). NGAM = non growth-associated ATP maintenance, HDCR = hydrogen dependent CO_2 reductase, CODH = CO dehydrogenase, Hyd = electron-bifurcating hydrogenase, Rnf = *Rhodobacter* nitrogen fixation complex, Fd_{red} = reduced ferredoxin, Fd_{ox} = oxidized ferredoxin. (For interpretation of the references to colour in this figure legend, the reader is referred to the web version of this article.)

towards a desired direction (ATP and biomass versus acetate formation). This strategy could also be applied to other gas fermenting organisms to control product spectra and shift production towards a desired target compound.

4. Conclusion

In this study, the effect of different gas compositions and mass transfer rates on CO_2 utilization, growth, and acetate production were characterized in batch and continuous cultures of *A. woodii*. Blending industrial BFG with H_2 enabled co-utilization of CO, CO_2 and H_2 and net CO_2 fixation at high CO and H_2 partial pressures. This strategy allowed to control CO_2 fixation, gas uptake and metabolic fluxes in continuous cultures. Its flexibility with respect to the utilization of gases at varying compositions makes *A. woodii* a very promising host for the reduction of industrial CO_2 emissions, even in CO-containing gases.

Funding

KN (#858702), CN (#874503) and SP (#858702, #874503) received funding from the Austrian Research Promotion Agency (FFG).

CRediT authorship contribution statement

Katharina Novak: Investigation, Data curation, Formal analysis, Conceptualization, Writing - original draft, Visualization. **Christian Neuendorf:** Investigation. **Irmela Kofler:** Resources, Investigation. **Nina Kieberger:** Resources, Investigation. **Steffen Klamt:** Formal analysis, Resources, Software. **Stefan Pflügl:** Conceptualization, Formal analysis, Resources, Writing - original draft, Supervision, Project administration, Funding acquisition.

Declaration of Competing Interest

The authors declare the following financial interests/personal relationships which may be considered as potential competing interests: Nina Kieberger is an employee of voestalpine Stahl GmbH. Voestalpine Stahl GmbH has interest to reduce its CO_2 emissions by recycling the carbon via gas fermentation for further use in products. All other authors declare that they have no competing interests.

Acknowledgements

The authors are indebted to Christoph Herwig for fruitful discussions and critical reading of the manuscript and Erwin Rosenberg for support with the GC system. We would like to thank Thomas Mainka and Samuele Verra for excellent technical assistance. voestalpine Stahl GmbH and OMV AG are gratefully acknowledged for financial support and the Austrian Research Promotion Agency (FFG) for funding. The authors acknowledge TU Wien Bibliothek for financial support through its Open Access Funding Program.

Appendix A. Supplementary data

Supplementary data to this article can be found online at https://doi.org/10.1016/j.biortech.2020.124573.

References

Arantes, A.L., Moreira, J.P.C., Diender, M., Parshina, S.N., Stams, A.J.M., Alves, M.M., Alves, J.I., Sousa, D.Z., 2020. Enrichment of anaerobic syngas-converting communities and isolation of a novel carboxydotrophic Acetobacterium wieringae Strain JM. Front. Microbiol. 11, 58. https://doi.org/10.3389/fmicb.2020.00058.

Bengelsdorf, F.R., Dürre, P., 2017. Gas fermentation for commodity chemicals and fuels. Microb. Biotechnol. 10 (5), 1167–1170. https://doi.org/10.1111/1751-7915.12763.

Bertsch, J., Müller, V., 2015a. Bioenergetic constraints for conversion of syngas to biofuels in acetogenic bacteria. Biotechnol. Biofuels 8 (1). https://doi.org/10.1186/s13068-015-0393-x.

Bertsch, J., Müller, V., 2015b. CO Metabolism in the Acetogen Acetobacterium woodii. Appl. Environ. Microbiol. 81 (17), 5949–5956. https://doi.org/10.1128/AEM.01772-15.

Cotter, J.L., Chinn, M.S., Grunden, A.M., 2009. Influence of process parameters on growth of Clostridium ljungdahlii and Clostridium autoethanogenum on synthesis gas. Enzyme Microb. Technol. 44 (5), 281–288. https://doi.org/10.1016/j.enzmictec.2008.11.002.

Das, D., Veziroglu, T., 2008. Advances in biological hydrogen production processes. Int. J. Hydrogen Energy 33 (21), 6046–6057. https://doi.org/10.1016/j.ijhydene.2008.07.098.

Demler, M., Weuster-Botz, D., 2011. Reaction engineering analysis of hydrogenotrophic production of acetic acid by Acetobacterium woodii. Biotechnol. Bioeng. 108 (2), 470–474. https://doi.org/10.1002/bit.22935.

Drake, H.L., Daniel, S.L., Küsel, K., Matthies, C., Kuhner, C., Braus-Stromeyer, S., 1997. Acetogenic bacteria: what are the in situ consequences of their diverse metabolic versatilities? BioFactors 6 (1), 13–24. https://doi.org/10.1002/biof.5520060103.

Erian, A.M., Gibisch, M., Pflügl, S., 2018. Engineered E. coli W enables efficient 2,3-butanediol production from glucose and sugar beet molasses using defined minimal medium as economic basis. Microb. Cell Fact. 17 (1) https://doi.org/10.1186/s12934-018-1038-0.

Eurostat [WWW Document], 2018. URL https://ec.europa.eu/eurostat/databrowser/view/ENV_AIR_GGE_custom_320301/default/table?lang=en (accessed 12.7.20).

Genthner, B.R.S., Bryant, M.P., 1987. Additional characteristics of one-carbon-compound utilization by Eubacterium limosum and Acetobacterium woodii. Appl. Environ. Microbiol. 53, 471–476.

Godley, AndrewR., Linnett, PaulE., Robinson, JohnP., 1990. The effect of carbon dioxide on the growth kinetics of fructose-limited chemostat cultures of Acetobacterium woodii DSM 1030. Arch. Microbiol. 154 (1) https://doi.org/10.1007/BF00249170.

Hallenbeck, P.C., Ghosh, D., 2009. Advances in fermentative biohydrogen production: the way forward? Trends Biotechnol. 27 (5), 287–297. https://doi.org/10.1016/j.tibtech.2009.02.004.

Heffernan, J.K., Valgepea, K., de Souza Pinto Lemgruber, R., Casini, I., Plan, M., Tappel, R., Simpson, S.D., Köpke, M., Nielsen, L.K., Marcellin, E., 2020. Enhancing CO2-valorization using clostridium autoethanogenum for sustainable fuel and chemicals production. Front. Bioeng. Biotechnol. 8, 204. https://doi.org/10.3389/fbioe.2020.00204.

Hermann, M., Teleki, A., Weitz, S., Niess, A., Freund, A., Bengelsdorf, F.R., Takors, R., 2020. Electron availability in CO2 , CO and H2 mixtures constrains flux distribution, energy management and product formation in Clostridium ljungdahlii. Microb. Biotechnol. 13 (6), 1831–1846. https://doi.org/10.1111/1751-7915.13625.

Hou, S.S., Chen, C.H., Chang, C.Y., Wu, C.W., Ou, J.J., Lin, T.H., 2011. Firing blast furnace gas without support fuel in steel mill boilers. Energy Convers. Manage. 52 (7), 2758–2767. https://doi.org/10.1016/j.enconman.2011.02.009.

Hungate, R.E., 1969. Chapter IV A roll tube method for cultivation of strict anaerobes. In: Norris, J.R., Ribbons, D.W. (Eds.), Methods in Microbiology. Academic Press, pp. 117–132. https://doi.org/10.1016/S0580-9517(08)70503-8.

Kantzow, C., Mayer, A., Weuster-Botz, D., 2015. Continuous gas fermentation by Acetobacterium woodii in a submerged membrane reactor with full cell retention. J. Biotechnol. 212, 11–18. https://doi.org/10.1016/j.jbiotec.2015.07.020.

Klamt, S., Saez-Rodriguez, J., Gilles, E.D., 2007. Structural and functional analysis of cellular networks with CellNetAnalyzer. BMC Syst. Biol. 1 (1) https://doi.org/10.1186/1752-0509-1-2.

Koch, S., Kohrs, F., Lahmann, P., Bissinger, T., Wendschuh, S., Benndorf, D., Reichl, U., Klamt, S., 2019. RedCom: A strategy for reduced metabolic modeling of complex microbial communities and its application for analyzing experimental datasets from anaerobic digestion. PLoS Comput. Biol. 15, e1006759. https://doi.org/10.1371/journal.pcbi.1006759.

Köpke, M., Simpson, S.D., 2020. Pollution to products: recycling of 'above ground' carbon by gas fermentation. Curr. Opin. Biotechnol. 65, 180–189. https://doi.org/10.1016/j.copbio.2020.02.017.

Liew, F., Henstra, A.M., Winzer, K., Köpke, M., Simpson, S.D., Minton, N.P., 2016a. Insights into CO 2 Fixation Pathway of Clostridium autoethanogenum by Targeted Mutagenesis. mBio 7 (3). https://doi.org/10.1128/mBio.00427-16.

Liew, F., Martin, M.E., Tappel, R.C., Heijstra, B.D., Mihalcea, C., Köpke, M., 2016b. Gas fermentation—A flexible platform for commercial scale production of low-carbon-fuels and chemicals from waste and renewable feedstocks. Front. Microbiol. 7 https://doi.org/10.3389/fmicb.2016.00694.

Mahamkali, V., Valgepea, K., de Souza Pinto Lemgruber, R., Plan, M., Tappel, R., Köpke, M., Simpson, S.D., Nielsen, L.K., Marcellin, E., 2020. Redox controls metabolic robustness in the gas-fermenting acetogen Clostridium autoethanogenum. PNAS 117 (23), 13168–13175. https://doi.org/10.1073/pnas.1919531117.

Mock, J., Zheng, Y., Mueller, A.P., Ly, S., Tran, L., Segovia, S., Nagaraju, S., Köpke, M., Dürre, P., Thauer, R.K., Metcalf, W.W., 2015. Energy Conservation Associated with Ethanol Formation from H 2 and CO 2 in Clostridium autoethanogenum Involving Electron Bifurcation. J. Bacteriol. 197 (18), 2965–2980. https://doi.org/10.1128/JB.00399-15.

Mohammadi, M., Younesi, H., Najafpour, G., Mohamed, A.R., 2012. Sustainable ethanol fermentation from synthesis gas by Clostridium ljungdahlii in a continuous stirred tank bioreactor. J. Chem. Technol. Biotechnol. 87 (6), 837–843. https://doi.org/10.1002/jctb.3712.

Molitor, B., Richter, H., Martin, M.E., Jensen, R.O., Juminaga, A., Mihalcea, C., Angenent, L.T., 2016. Carbon recovery by fermentation of CO-rich off gases – Turning steel mills into biorefineries. Bioresour. Technol. 215, 386–396. https://doi.org/10.1016/j.biortech.2016.03.094.

Munasinghe, P.C., Khanal, S.K., 2010. Biomass-derived syngas fermentation into biofuels: Opportunities and challenges. Bioresour. Technol. 101 (13), 5013–5022. https://doi.org/10.1016/j.biortech.2009.12.098.

Novak, K., Kutscha, R., Pflügl, S., 2020. Microbial upgrading of acetate into 2,3-butanediol and acetoin by E. coli W. Biotechnol. Biofuels 13 (1). https://doi.org/10.1186/s13068-020-01816-7.

Novak, K., Pflügl, S., 2018. Towards biobased industry: acetate as a promising feedstock to enhance the potential of microbial cell factories. FEMS Microbiol. Lett. 365 https://doi.org/10.1093/femsle/fny226.

Pardo, N., Moya, J.A., 2013. Prospective scenarios on energy efficiency and CO2 emissions in the European Iron & Steel industry. Energy 54, 113–128. https://doi.org/10.1016/j.energy.2013.03.015.

Ragsdale, S.W., Ljungdahl, L.G., 1984. Hydrogenase from Acetobacterium woodii. Arch. Microbiol. 139 (4), 361–365. https://doi.org/10.1007/BF00408380.

Ragsdale, S.W., Ljungdahl, L.G., Dervartanian, D.V., 1983. Isolation of Carbon Monoxide Dehydrogenase from Acetobacterium woodii and Comparison of Its Properties with Those of the Clostridium thermoaceticum Enzyme. J. Bacteriol. 155, 14.

Rittmann, S., Seifert, A., Herwig, C., 2012. Quantitative analysis of media dilution rate effects on Methanothermobacter marburgensis grown in continuous culture on H2 and CO2. Biomass Bioenergy 36, 293–301. https://doi.org/10.1016/j.biombioe.2011.10.038.

Schoelmerich, M.C., Müller, V., 2020. Energy-converting hydrogenases: the link between H2 metabolism and energy conservation. Cell. Mol. Life Sci. 77 (8), 1461–1481. https://doi.org/10.1007/s00018-019-03329-5.

Schuchmann, K., Müller, V., Stams, A.J.M., 2016. Energetics and application of heterotrophy in acetogenic bacteria. Appl. Environ. Microbiol. 82 (14), 4056–4069. https://doi.org/10.1128/AEM.00882-16.

Schuchmann, K., Müller, V., 2014. Autotrophy at the thermodynamic limit of life: a model for energy conservation in acetogenic bacteria. Nat. Rev. Microbiol. 12 (12), 809–821. https://doi.org/10.1038/nrmicro3365.

Schwarz, F.M., Ciurus, S., Jain, S., Baum, C., Wiechmann, A., Basen, M., Müller, V., 2020. Revealing formate production from carbon monoxide in wild type and mutants of Rnf- and Ech-containing acetogens, *Acetobacterium woodii* and *Thermoanaerobacter kivui*. Microb. Biotechnol. 13 (6), 2044–2056. https://doi.org/10.1111/1751-7915.13663.

Schwarz, F.M., Müller, V., 2020. Whole-cell biocatalysis for hydrogen storage and syngas conversion to formate using a thermophilic acetogen. Biotechnol. Biofuels 13 (1). https://doi.org/10.1186/s13068-020-1670-x.

Takors, R., Kopf, M., Mampel, J., Bluemke, W., Blombach, B., Eikmanns, B., Bengelsdorf, F.R., Weuster-Botz, D., Dürre, P., 2018. Using gas mixtures of CO, CO 2 and H 2 as microbial substrates: the do's and don'ts of successful technology transfer from laboratory to production scale. Microb. Biotechnol. 11 (4), 606–625. https://doi.org/10.1111/1751-7915.13270.

Valgepea, K., de Souza Pinto Lemgruber, R., Abdalla, T., Binos, S., Takemori, N., Takemori, A., Tanaka, Y., Tappel, R., Köpke, M., Simpson, S.D., Nielsen, L.K., Marcellin, E., 2018. H2 drives metabolic rearrangements in gas-fermenting Clostridium autoethanogenum. Biotechnol. Biofuels 11 (1). https://doi.org/10.1186/s13068-018-1052-9.

Valgepea, K., de Souza Pinto Lemgruber, R., Meaghan, K., Palfreyman, R.W., Abdalla, T., Heijstra, B.D., Behrendorff, J.B., Tappel, R., Köpke, M., Simpson, S.D., Nielsen, L.K., Marcellin, E., 2017. Maintenance of ATP Homeostasis Triggers Metabolic Shifts in Gas-Fermenting Acetogens. Cell Systems 4 (5), 505–515.e5. https://doi.org/10.1016/j.cels.2017.04.008.

Vees, C.A., Neuendorf, C.S., Pflügl, S., 2020. Towards continuous industrial bioprocessing with solventogenic and acetogenic clostridia: challenges, progress and perspectives. J. Ind. Microbiol. Biotechnol. 47 (9-10), 753–787. https://doi.org/10.1007/s10295-020-02296-2.

von Kamp, A., Thiele, S., Hädicke, O., Klamt, S., 2017. Use of CellNetAnalyzer in biotechnology and metabolic engineering. J. Biotechnol. 261, 221–228. https://doi.org/10.1016/j.jbiotec.2017.05.001.

Weghoff, M.C., Müller, V., Liu, S.-J., 2016. CO Metabolism in the Thermophilic Acetogen Thermoanaerobacter kivui. Appl. Environ. Microbiol. 82 (8), 2312–2319. https://doi.org/10.1128/AEM.00122-16.

Westphal, L., Wiechmann, A., Baker, J., Minton, N.P., Müller, V., 2018. The Rnf complex is an energy-coupled transhydrogenase essential to reversibly link cellular NADH and Ferredoxin pools in the acetogen Acetobacterium woodii. J. Bacteriol. 200 https://doi.org/10.1128/JB.00357-18.

Wiechmann, A., Ciurus, S., Oswald, F., Seiler, V.N., Müller, V., 2020. It does not always take two to tango: "Syntrophy" via hydrogen cycling in one bacterial cell. ISME J. 14 (6), 1561–1570. https://doi.org/10.1038/s41396-020-0627-1.

Yukesh Kannah, R., Kavitha, S., Preethi, Parthiba Karthikeyan, O., Kumar, G., Dai-Viet, N.V., Rajesh Banu, J., 2021. Techno-economic assessment of various hydrogen production methods – A review. Bioresour. Technol. 319, 124175. https://doi.org/10.1016/j.biortech.2020.124175.